Performance improvement of MEH-PPV:PCBM solar cells using bathocuproine and bathophenanthroline as the buffer layers*

Liu Xiao-Dong(刘晓东), Zhao Su-Ling (赵谡玲)†, Xu Zheng(徐 征), Zhang Fu-Jun(张福俊), Zhang Tian-Hui(张天慧), Gong Wei(龚 伟), Yan Guang(闫 光), Kong Chao(孔 超), Wang Yong-Sheng(王永生), and Xu Xu-Rong(徐叙瑢)

Key Laboratory of Luminescence and Optical Information of Ministry of Education, Beijing Jiaotong University, Beijing 100044, *China*

(Received 29 November 2010; revised manuscript received 13 January 2011)

In this work, bathocuproine (BCP) and bathophenanthroline (Bphen), commonly used in small-molecule organic solar cells (OSCs), are adopted as the buffer layers to improve the performance of the polymer solar cells (PSCs) based on poly(2-methoxy-5-(2-ethylhexyloxy)-1,4-phenylenevinylene) (MEH-PPV): [6,6]-phenyl-C_{61}-butyric acid methyl ester (PCBM) bulk heterojunction. By inserting BCP or Bphen between the active layer and the top cathode, all the performance parameters are dramatically improved. The power conversion efficiency is increased by about 70% and 120% with 5-nm BCP and 12-nm Bphen layers, respectively, when compared with that of the devices without any buffer layer. The performance enhancement is attributed to BCP or Bphen (i) increasing the optical field, and hence the absorption in the active layer, (ii) effectively blocking the excitons generated in MEH-PPV from quenching at organic/aluminum (Al) interface due to the large band-gap of BCP or Bphen, which results in a significant reduction in series resistance (R_s), and (iii) preventing damage to the active layer during the metal deposition. Compared with the traditional device using LiF as the buffer layer, the BCP-based devices show a comparable efficiency, while the Bphen-based devices show a much larger efficiency. This is due to the higher electron mobility in Bphen than that in BCP, which facilitates the electron transport and extraction through the buffer layer to the cathode.

Keywords: polymer solar cells, bathocuproine, bathophenanthroline, buffer layer

PACS: 88.40.jr, 71.20.Rv, 79.60.Jv **DOI:** 10.1088/1674-1056/20/6/068801

1. Introduction

Polymer solar cells (PSCs), considered as a promising source of renewable energy, have attracted much attention because of their low-cost, compatibility with flexible substrates and large-area applications.[1−4] Recently, the power conversion efficiency (PCE $\equiv \eta$) of the bulk heterojunction (BHJ) PSCs around 7% has been realized.[5,6] However, compared with their inorganic semiconductor counterparts, the efficiency is still low and not yet sufficient for commercial implementation, for which an efficiency of 10% is expected to be a minimum requirement. To further improve PCE, it is proved that the introduction of a buffer layer between the organic and the electrode layers is an effective approach.[7−11] At present, a thin layer of LiF is commonly used as the buffer layer to modify the interface between the active layer and the cathode in PSCs.[12,13] As we know, LiF is an insulating material, so the thickness must be strictly controlled in order to prevent a thicker LiF layer from being detrimental to electron collection (generally lower than 1.5 nm). For bilayer organic solar cells (OSCs) based on small-molecule materials, bathocuproine (BCP) is usually used as an exciton-blocking layer (EBL) due to its high band-gap.[14] In addition, Chan *et al.*[15] reported that bathophenanthroline (Bphen) may be a better alternative compared with BCP because of its higher electron transporting ability. In this paper, we use these two materials, BCP and Bphen, respectively, as substitutes for LiF in buffer layers in PSCs based on a poly(2-methoxy-5-(2-ethylhexyloxy)-

*Project supported by the National Natural Science Foundation of China (Grant Nos. 60978060, 10804006, and 10974013), the Research Fund for the Doctoral Program of Higher Education of China (Grant No. 20090009110027), the Research Fund for the Youth Scholars of the Doctoral Program of Higher Education, China (Grant No. 20070004031), the Beijing Municipal Natural Science Foundation of China (Grant No. 1102028), the Beijing Municipal Science & Technology Commission of China (Grant No. Z090803044009001), the National Basic Research Program of China (Grant No. 2010CB327705), and the International Science and Technology Cooperation Program (Grant No. 2008DFA61420).

†Corresponding author. E-mail: slzhao@bjtu.edu.cn

© 2011 Chinese Physical Society and IOP Publishing Ltd

1,4-phenylenevinylene) (MEH-PPV) and [6,6]-phenyl-C_{61}-butyric acid methyl ester (PCBM) blend. Both BCP and Bphen can noticeably improve the performance of PSCs. Compared with the device using LiF as a buffer layer, the BCP-based devices show a comparable efficiency, while the Bphen-based devices show a much better efficiency, which may be attributed to the higher electron mobility in Bphen than that in BCP.

2. Experiment

All the devices in this work were fabricated on indium tin oxide (ITO)-coated glass substrates, which had been carefully cleaned by acetone, ethanol and de-ionized water consecutively, and finally dried by blowing with nitrogen gas and baking at 80 °C for 5 min in air. After the dried ITO glass substrates were treated by UV ozone for 10 min, the filtered poly(3,4-ethylenedioxythiophene):poly(styrenesulfonate) (PEDOT:PSS) was spin coated on the top of the ITO surface with a speed of 2000 rpm (round per minute) for 50 s and then annealed in a vacuum at 120 °C for 10 min. The MEH-PPV:PCBM, dissolved in chlorobenzene with a weight ratio of 1:4, was spin coated onto the PEDOT:PSS layer at the same speed of 2000 rpm. Layers of Bphen, BCP, LiF and an aluminum (Al) electrode were thermally evapourated under high vacuum. Deposition rates were monitored with a quartz oscillating crystal and controlled to be 1 Å/s for both organic layers and LiF. A shadow mask was used for the deposition of the cathode, giving an active device area of 0.1 cm^2. Figure 1 shows the device configuration of organic photovoltaic cells used in the study.

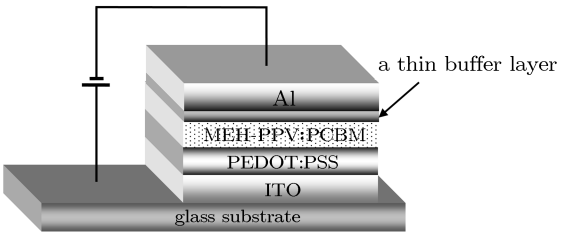


Fig. 1. Schematic device structure of organic solar cells.

All the experiments in this paper were divided into several groups due to the limitation of our evaporation equipment where only four devices can be fabricated at once. So the device without any buffer layer was fabricated and acted as a reference for comparison in each group. The minor variation of the PCE, mainly caused by fill factor (FF), for the reference devices with the same structure cannot influence our experimental trends.

The current–voltage (I–V) curves were measured with a Keithley 2410 source-measurement unit in the dark and under illumination of 150-W xenon lamp at an intensity of 100 mW/cm^2. The absorption spectra of the organic films were recorded by Shimadzu UV-3101 PC spectrometer. All the measurements were carried out in air at room temperature.

3. Results and discussion

Figure 2 shows the absorption spectra of MEH-PPV, PCBM, BCP and Bphen films on quartz substrates. Obviously, both the BCP and the Bphen films have nearly negligible absorbances as compared with those of the photoactive MEH-PPV and PCBM films, so that the buffer layers do not absorb the light reflected from the cathode. On the other hand, a thin film between the active layer and the electrode is usually used as an optical spacer to redistribute the light intensity.[3,16] With this consideration, we simulate the optical field distribution for a single wavelength illumination (500 nm, corresponding to the MEH-PPV absorption peak) in the PSCs with different thicknesses of BCP or Bphen (the same refractive index, 1.75[17,18] at λ = 500 nm, for both BCP and Bphen due to their similar optical properties). The simulation result is shown in Fig. 3. It can be seen that the position of the maximum peak shifts toward the centre of the active layer and the relative optical intensity is enhanced with the increase of the BCP (or Bphen) thickness. High optical field intensity in the active layer results in high optical absorption, therefore we anticipate that this enhanced optical intensity will lead to the increase of the short-circuit current density (J_{sc}), and thus the PCE.

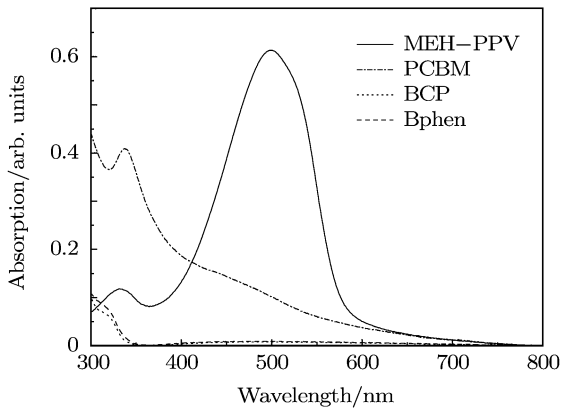


Fig. 2. Absorption spectra of MEH-PPV (solid), PCBM (dash-dot), BCP (dot), and Bphen (dash).

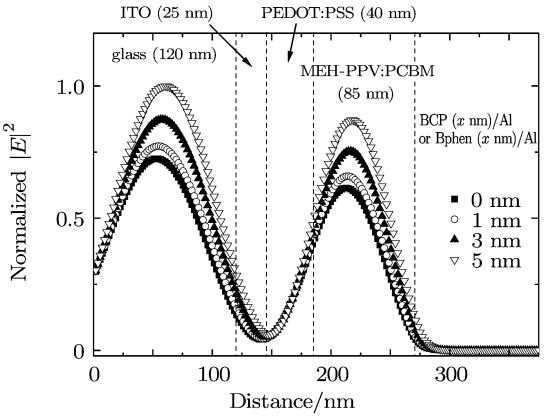


Fig. 3. Simulated optical field distributions (for 500-nm illumination) each as a function of the position in the Glass/ITO (25 nm)/PEDOT:PSS (40 nm)/MEH-PPV:PCBM (85 nm)/BCP or Bphen (0, 1, 3, 5 nm)/Al (100 nm) PSCs. The refractive indices of glass, ITO, PEDOT:PSS, MEH-PPV:PCBM, BCP (or Bphen), Al layers are 1.42, 1.92, 1.50+0.02i, 1.81+0.13i, 1.75, and 0.82+6.02i, respectively, at $\lambda = 500$ nm.

3.1. Introduction of BCP as the buffer layer

For small-molecule OSCs, BCP is commonly used as a buffer layer between the acceptor and the top cathode due to its large energy gap (3.5 eV).[8,14] Here, this small-molecular-weight material is used to improve the performance of PSCs based on MEH-PPV and PCBM blend. Figure 4 shows the current density–voltage (J–V) characteristics of the devices with the thickness of BCP ranging from 0 to 5 nm under an illumination of 100 mW/cm^2. The device without the BCP layer has a poor performance: $J_{sc} = 2.25$ mA/cm, open-circuit voltage (V_{oc})=0.71 V, and FF=36.4%. The calculated η is equal to 0.58% ($\eta = J_{sc}V_{oc}\mathrm{FF}/P_{inc}$, where P_{inc} is the incident light power density). After inserting a thin BCP buffer layer between MEH-PPV:PCBM and Al layers, all the performance parameters are improved. When the thickness of BCP film is 5 nm, the device exhibits a good performance with $J_{sc} = 2.95$ mA/cm^2, $V_{oc} = 0.75$ V, and FF=44.1%. The corresponding η is 0.98%, which has a 69% increase over that of the device without BCP. This significant improvement is attributed to the following effects: (i) as an optical spacer, BCP increases the light absorption in the active layer by redistributing the optical field inside the device; (ii) as an EBL, BCP effectively blocks the excitons generated in MEH-PPV from cathode quenching. The confinement of excitons can increase the probability of exciton dissociation at MEH-PPV/PCBM interface and thereby leads to a high photocurrent;[15] (iii) as a protection layer, BCP prevents the underlying layer from deteriorating during Al deposition.[8,16,19] Table 1 summarizes the key photovoltaic parameters as a function of BCP thickness under illumination.

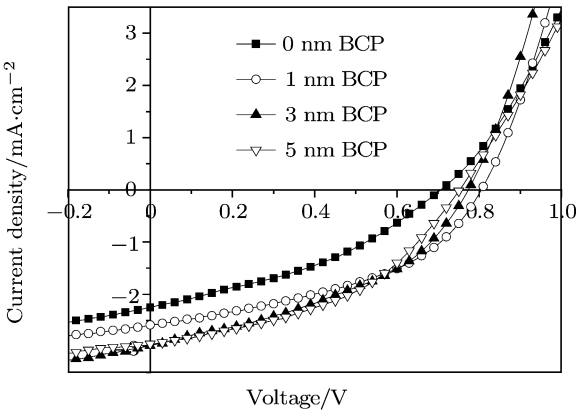


Fig. 4. The J–V characteristics for the devices with different thicknesses (0, 1, 3, 5 nm) of BCP under illumination at 100 mW/cm^2.

Table 1. Key parameters for organic photovoltaic devices with different thicknesses (0, 1, 3, 5 nm) of BCP as the buffer layer.

BCP/nm	J_{sc}/mA·cm^{-2}	V_{oc}/V	FF/%	η/%	R_s/Ω
0	2.25	0.71	36.4	0.58	1253.5
1	2.59	0.81	43.7	0.92	538.6
3	2.99	0.77	41.1	0.95	547.2
5	2.95	0.75	44.1	0.98	840.2

3.2. Introduction of Bphen as the buffer layer

BCP easily crystallizes when exposed to the atmosphere environment due to the presence of water and oxygen.[20] Chan *et al.*[15] and Wang *et al.*[21] proposed another effective EBL Bphen which has similar electrical and optical properties but better water withstanding and oxygen blocking abilities as compared with those of BCP. In this paper, another group of

devices with the same structure as above (see Fig. 1), but in which Bphen is adopted to replace BCP as the buffer layer, were fabricated. Figure 5 shows the J–V characteristics of the devices without and with Bphen modification. The Bphen thickness also varies from 0 to 5 nm. The device with no buffer layer shows a similar performance to that in Fig. 4. By modifying the Al cathode by 5-nm Bphen provides a significant improvement on the device performance where J_{sc} increases to 3.98 mA/cm^2, V_{oc} to 0.74 V, and FF to 44.3%. The corresponding η reaches up to 1.30%, which has a 95% increase as compared with that of the device without any buffer layer. Table 2 shows the key parameters for the devices with different thicknesses (0, 1, 3, 5 nm) of Bphen. It is worthwhile noting that Bphen-based devices show a better performance than that of BCP-based devices. The reason will be discussed in Subsection 3.3.

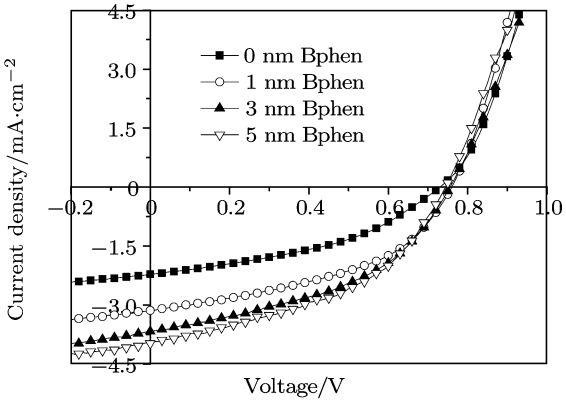


Fig. 5. Illuminated J–V characteristics for the devices with different thicknesses (0, 1, 3, 5 nm) of Bphen.

Table 2. Key parameters for organic photovoltaic devices with different thicknesses (0, 1, 3, 5 nm) of Bphen as the buffer layer.

Bphen/nm	J_{sc}/mA·cm^{-2}	V_{oc}/V	FF/%	η/%	R_s/Ω
0	2.22	0.73	41.3	0.67	763.4
1	3.14	0.76	45.3	1.08	382.4
3	3.67	0.76	44.1	1.23	455.7
5	3.98	0.74	44.3	1.30	424.1

3.3. Comparison between BCP and Bphen as the buffer layers

Figure 6 shows the variations of J_{sc}, V_{oc} (a), FF, and PCE (b) each as a function of Bphen and BCP thicknesses. It can be clearly seen that the J_{sc} of BCP-based device first increases and then drops with the thickness of BCP buffer layer, while that of Bphen-based devices increases monotonically with the thickness of Bphen. J_{sc} depends on the light absorption as well as the carrier transport after exciton separation into free charges.[22] As discussed in the beginning, BCP (or Bphen) increases the absorption in the active layer due to the redistribution of the light intensity. On the other hand, the insertion of a nanometer buffer layer may result in the formation of a better Ohmic contact and consequently lower the series resistance (R_s) of the device. From the illuminated J–V characteristics in Figs. 4 and 5, we evaluate the specific R_s, which is given by the inverse gradient of the J–V curve at 0 mA/cm^2. As shown in Tables 1 and 2, the R_s decreases from 1253.5 Ω to 538.6 Ω and from 763.4 Ω to 382.4 Ω when the reference devices are modified by 1-nm BCP and 1-nm Bphen, respectively. This demonstrates that both BCP and Bphen can improve the polymer/Al interface efficiently. However, as the BCP thickness increases to 5 nm, the R_s has a sharp increase, leading to a slight drop in J_{sc}. As shown in Fig. 7,[21,23] it appears that the photogenerated electrons are difficult to transport from the lowest unoccupied molecular orbital (LUMO) of PCBM to an Al cathode because of the large barrier formed by the EBL LUMO, which is at least 0.8 eV for both BCP and Bphen. Peumans and Forrest[14] suggested that electron transport in the BCP EBL occurs mainly through defect states induced by the hot metal atoms during cathode deposition. Based on this hypothesis, it is believed that for a thicker BCP, the region far from the BCP/Al interface has insufficient defect states for carrier transport, thereby leading to a lower electron mobility μ_e in the BCP layer (μ_e is proportional to the defect state density), and thus, an increased R_s. In contrast to BCP, the device with 5-nm Bphen as the EBL still yields a small R_s. Moreover, the Bphen-based devices show the better performance over that of the BCP-based devices (the maximum PCE of 1.30% and 0.98% for the Bphen and BCP based devices, respectively). Those can be explained by the fact that μ_e of Bphen (5.0×10^{-4} cm^2·V^{-1}·s^{-1})[24] is two orders of magnitude higher than that of BCP (5.0×10^{-6} cm^2·V^{-1}·s^{-1}).[23] The much higher μ_e facilitates the electron transport and extraction, and

thereby results in a larger J_{sc}, which is in agreement with the experimental data (see Tables 1 and 2).

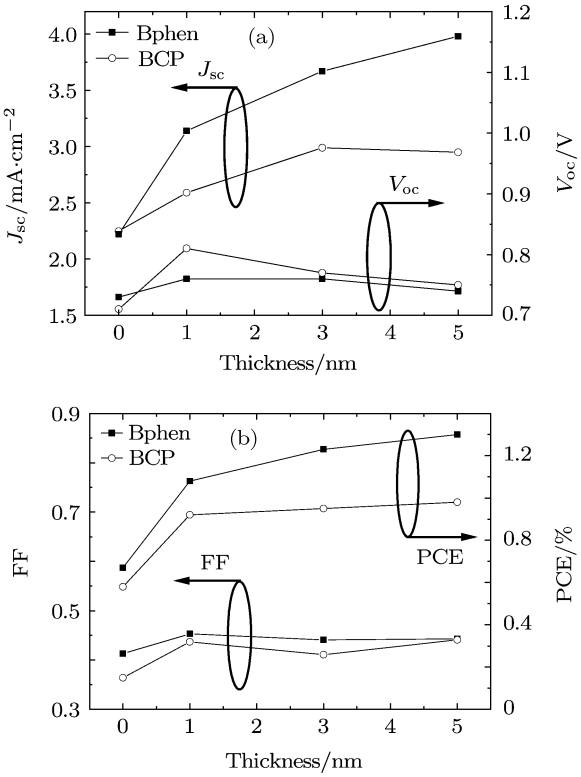


Fig. 6. Variations of J_{sc}, V_{oc} (a), FF and PCE (b) with Bphen (■) and BCP (◯) thicknesses.

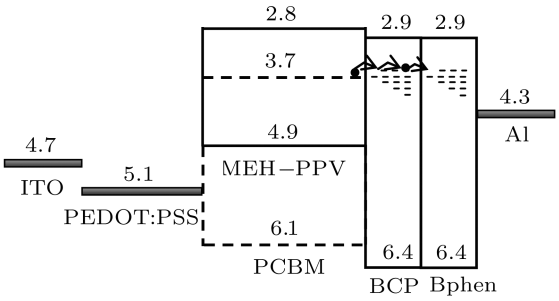


Fig. 7. Energy level diagram of the modified photovoltaic device.

As a buffer layer, there must be an optimized thickness due to the reduction of electron mobility with the thickness increasing. Considering this, we continue to increase the thickness of Bphen from 8 nm to 15 nm. A device without Bphen was also fabricated and acted as a reference for comparison. Figure 8 shows the J–V characteristics of the devices with different thicknesses (0, 8, 12, 15 nm) of Bphen. The key parameters of these PSCs are summarized in Table 3. The performance of the reference device is slightly higher than those in Figs. 4 and 5. It can be clearly seen that J_{sc} first increases to a maximum of 3.99 mA/cm^2 as the Bphen thickness increases to 12 nm and then decreases as the Bphen buffer layer becomes thicker. Furthermore, the R_s also has an abrupt increase when the thickness of Bphen reaches 15 nm (see Table 3). The interpretation of these results is similar to that of BCP-based devices. Additionally, it should be especially noted that at the optimum thickness of Bphen (12 nm), the η reaches to 1.73%, which is a more-than-twofold increase as compared with that of the reference device.

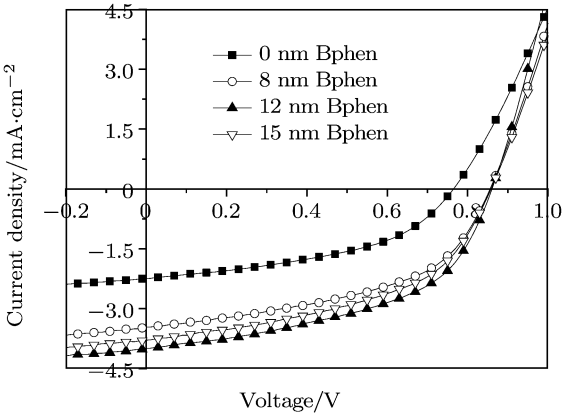


Fig. 8. Illuminated J–V characteristics for the devices with different thicknesses (0, 8, 12, 15 nm) of Bphen.

Table 3. Key parameters for organic photovoltaic devices with different thicknesses (0, 8, 12, 15 nm) of Bphen as the buffer layer.

Bphen/nm	J_{sc}/mA·cm^{-2}	V_{oc}/V	FF/%	η/%	R_s/Ω
0	2.25	0.76	46.6	0.80	620.9
8	3.47	0.86	49.4	1.47	362.8
12	3.99	0.86	50.4	1.73	295.8
15	3.79	0.86	48.8	1.59	377.4

3.4. Comparison between LiF and organic materials as the buffer layers

Finally, a device with 1-nm LiF commonly used in PSCs was fabricated for comparison. Figure 9 shows the J–V characteristics of devices with 1-nm LiF, 5-nm BCP and 12-nm Bphen (the optimum thicknesses for BCP and Bphen based devices, respectively). The device with 1-nm LiF exhibits a J_{sc} of 2.89 mA/cm^2, a V_{oc} of 0.7 V, an FF of 49.1%,

and a η of 0.99%, which is comparable to that of 5-nm BCP-based device (0.98%), but lower than that of 12-nm Bphen-based device (1.73%). The results suggest that Bphen is the best choice as the buffer layer in PSCs due to its large energy gap and high electron mobility.

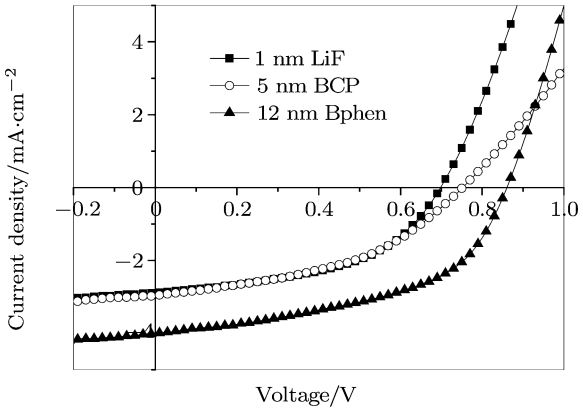


Fig. 9. Illuminated J–V characteristics of devices with 1-nm LiF (■), 5-nm BCP (◯), and 12-nm Bphen (▲) as the buffer layers.

4. Conclusion

We investigated the effects of interfacial buffer layers—BCP and Bphen on the performance of polymer solar cells based on MEH-PPV and PCBM blend. After inserting 5-nm BCP and 12-nm Bphen between the active layer and the cathode, the PCE are substantially increased by a factor of 0.69 and 1.16, respectively, as compared with the devices without any buffer layer. The roles of BCP and Bphen might be the same for efficiency improvement because of their similar optical transparency and energy gap. However, compared with traditional devices by using LiF as the buffer layer, the BCP-based devices show a comparable efficiency, while Bphen-based devices show a much higher efficiency. This is due to the better electron transport ability of Bphen than that of BCP.

References

[1] Yu G, Gao J, Hummelen J C, Wudl F and Heeger A J 1995 *Science* **270** 1789
[2] Reyes-Reyes M, Kim K and Carroll D L 2005 *Appl. Phys. Lett.* **87** 083506
[3] Kim J Y, Lee K, Coates N E, Moses D, Nguyen T Q, Dante M and Heeger A J 2007 *Science* **317** 222
[4] Dennler G, Scharber M C and Brabec C J 2009 *Adv. Mater.* **21** 1323
[5] Chen H Y, Hou J H, Zhang S Q, Liang Y Y, Yang G W, Yang Y, Yu L P, Wu Y and Li G 2009 *Nature Photon.* **3** 649
[6] Liang Y Y, Xu Z, Xia J B, Tsai S T, Wu Y, Li G, Ray C and Yu L P 2010 *Adv. Mater.* **22** E135
[7] Li G, Chu C W, Shrotriya V, Huang J and Yang Y 2006 *Appl. Phys. Lett.* **88** 253503
[8] Song Q L, Li F Y, Yang H, Wu H R, Wang X Z, Zhou W, Zhao J M, Ding X M, Huang C H and Hou X Y 2005 *Chem. Phys. Lett.* **416** 42
[9] Kang B, Tan L W and Silva S R P 2008 *Appl. Phys. Lett.* **93** 133302
[10] Yoo I, Lee M, Lee C, Kim D W, Moon I S and Hwang D H 2005 *Synth. Met.* **153** 97
[11] Tao C, Ruan S P, Xie G H, Kong X Z, Shen L, Meng F X, Liu C X, Zhang X D, Dong W and Chen W Y 2009 *Appl. Phys. Lett.* **94** 043311
[12] Brabec C J, Shaheen S E, Winder C, Sariciftci N S and Denk P 2002 *Appl. Phys. Lett.* **80** 1288
[13] Kim M S, Kang M G, Guo L J and Kim J 2008 *Appl. Phys. Lett.* **92** 133301
[14] Peumans P and Forrest S R 2001 *Appl. Phys. Lett.* **79** 126
[15] Chan M Y, Lee C S, Lai S L, Fung M K, Wong F L, Sun H Y, Lau K M and Lee S T 2006 *J. Appl. Phys.* **100** 094506
[16] Zhao D W, Liu P, Sun X W, Tan S T, Ke L and Kyaw A K K 2009 *Appl. Phys. Lett.* **95** 153304
[17] Wu Z X, Wang L D, Lei G T and Qiu Y 2005 *J. Appl. Phys.* **97** 103105
[18] Liu Z T, Kwong C Y, Cheung C H, Djurišić A B, Chan Y and Chui P C 2005 *Synth. Met.* **150** 159
[19] Liu X D, Xu Z, Zhang F J, Zhao S L, Zhang T H, Gong W, Song J L, Kong C, Yan G and Xu X R 2010 *Chin. Phys.* B **19** 118601
[20] Peumans P, Yakimov A and Forrest S R 2003 *J. Appl. Phys.* **93** 3693
[21] Wang N N, Yu J S, Zang Y, Huang J and Jiang Y D 2010 *Sol. Energy Mater. Sol. Cells* **94** 263
[22] Zhang F, Ceder M and Inganäs O 2007 *Adv. Mater.* **19** 1835
[23] Ichikawa M, Amagai J, Horiba Y, Koyama T and Taniguchi Y 2003 *J. Appl. Phys.* **94** 7796
[24] Naka S, Okada H, Onnagawa H and Tsutsui T 2000 *Appl. Phys. Lett.* **76** 197